Environmental Science and Pollution Research
https://doi.org/10.1007/s11356-022-23300-5

CARBON-BASED NANOMATERIALS: SYSTEMATIC ENUMERATION AND PROFICIENT TEMPLATE FOR DETECTION AND REMEDIATION OF HAZARDOUS POLLUTANTS

Cost-effective screen-printed carbon electrode biosensors for rapid detection of microcystin-LR in surface waters for early warning of harmful algal blooms

Stephanie Stoll[1] · Jae-Hoon Hwang[1] · David W. Fox[2] · Keugtae Kim[3] · Lei Zhai[2] · Woo Hyoung Lee[1]

Received: 13 July 2022 / Accepted: 23 September 2022

Abstract
Microcystins (MCs) are toxins produced by cyanobacteria commonly found in harmful algal blooms (HABs). Due to their toxicity to humans and other organisms, the World Health Organization (WHO) sets a guideline of 1 μg L^{-1} for microcystin-leucine-arginine (MC-LR) in drinking water. However, current analytical techniques for the detection of MC-LR such as liquid chromatography-mass spectrometry (LC-MS) and ELISA are costly, bulky, time-consuming, and mostly conducted in a laboratory, requiring highly trained personnel. An analytical method that can be used in the field for rapid determination is essential. In this study, an anti-MC-LR/MC-LR/cysteamine-coated screen-printed carbon electrode (SPCE) biosensor was newly developed to detect MC-LR, bioelectrochemically, in water. The functionalization of the electrode surface was confirmed with surface characterization methods. The sensor performance was evaluated by electrochemical impedance spectroscopy (EIS), obtaining a linear working range of MC-LR concentrations between 0.1 and 100 μg L^{-1} with a limit of detection (*LOD*) of 0.69 ng L^{-1}. Natural water samples experiencing HABs were collected and analyzed using the developed biosensor, demonstrating the excellent performance of the biosensor with a relative standard deviation (RSD) of 0.65%. The interference tests showed minimal error and RSD values against other common MCs and possible coexisting ions found in water. The biosensor showed acceptable functionality with a shelf life of up to 12 weeks. Overall, the anti-MC-LR/MC-LR/cysteamine/SPCE biosensors can be an innovative solution with characteristics that allow for in situ, low-cost, and easy-to-use capabilities which are essential for developing an overarching and integrated "smart" environmental management system.

Keywords Antibody · Biosensor · Cyanobacteria · Harmful algal blooms (HABs) · MC-LR · Microcystin

Introduction

Freshwater and estuarine ecosystems that provide critical habitats for diverse species of flora and fauna while supporting recreational activities and tourism businesses are frequently threatened by the increasing occurrences of cyanobacterial harmful algal blooms (cyanoHABs). While cyanoHABs disrupt the balance of various life forms in aquatic ecosystems, cyanotoxins produced by cyanobacteria can endanger human and aquatic organisms at all taxonomy levels (Backer et al. 2015). Airborne and waterborne cyanotoxins may cause serious health problems for residents as well as economic losses throughout multiple segments of society (Dyson and Huppert 2010). Microcystins (MCs), also known as hepatotoxins, are the most common cyanotoxins associated with freshwater cyanoHABs. Human exposure

Responsible Editor: Lotfi Aleya

✉ Woo Hyoung Lee
WooHyoung.Lee@ucf.edu

[1] Department of Civil, Environmental, and Construction Engineering, University of Central Florida, Orlando, FL 32816, USA

[2] Nanoscience Technology Center and Department of Chemistry, University of Central Florida, Orlando, FL 32816, USA

[3] Department of Environmental and Energy Engineering, The University of Suwon, 17 Wauan-gil, Bongdam-eup, Hwaseong-si, Gyeonggi-do 18323, South Korea

Published online: 04 October 2022

to MCs can cause acute or chronic health hazards (Preece et al. 2017). The majority of states in the United States (US) and other countries have their own set of guidelines for these toxins (Poretti et al. 2020). The World Health Organization (WHO) set a guideline of 1 μg L^{-1} for MC-LR in drinking water and the US Environmental Protection Agency (EPA) recommends a recreational value of 8 μg L^{-1} (USEPA 2019).

It is important to monitor the occurrence of HABs and the concentrations of cyanotoxins which are being produced by cyanobacteria to warn people in the area to stay away if the level of MC-LR concentration becomes too high. There exist visual observation, hyperspectral images (HSI) sensors (Park et al. 2020), and satellite image-based tools for monitoring cyanoHABs. However, cyanotoxin production is highly variable regardless of the presence of cyanobacteria and toxins can occur at unsafe levels without a visual bloom. Traditionally, the presence of cyanotoxins at trace concentrations has been confirmed through time and resource-consuming methods which include liquid chromatography/tandem mass spectrometry (LC/MS/MS, EPA method 544) (Shoemaker 2015), high-performance liquid chromatography (HPLC, EPA method 8315A) (USEPA 1996), and enzyme-linked immunosorbent assay (ELISA, EPA method 546) (Zaffiro et al. 2016). These methods have a good detection range of 0.1 to 2.5 μg L^{-1}, but they are time-consuming and mostly conducted in a laboratory, often requiring expensive equipment and highly trained personnel. Therefore, it is urgent to develop a cost-effective, simple, and reliable cyanotoxin detecting tool to respond quickly during HAB events.

Biosensors have been proposed as an effective method to detect trace amounts of various emerging contaminants such as viruses (Pilevar et al. 2021), pharmaceuticals, antibiotics (Alipoori et al. 2021), and infectious diseases (Menon et al. 2020). Among many types of biosensors, bioelectrochemical detection can be a promising alternative to conventional methods due to its simplicity, readiness, and effectiveness. In bioelectrochemical MC-LR detection, the sensing technique heavily depends upon the affinity between the antibody and MC-LR molecules. It was previously discovered that MC-LR contains a unique structural feature, a β-amino acid (ADDA), which plays an important role in its toxicity as well as its recognition by ADDA-specific antibodies (Nagata et al. 1995). Many studies have reported the detection of MC-LR using monoclonal antibodies AD4G2 (Adamovský et al. 2011), IgG1 (e.g., mouse and goat) (Sheng et al. 2007), polyclonal antibodies (Campàs et al. 2007), and functionalized DNA-antibodies (Suo et al. 2021). However, most biosensors were fabricated using gold as a substrate or glass carbon electrodes (GCE) and often use nanoparticles to increase the sensitivity (Bilibana et al. 2016; Hou et al. 2016; Zhang et al. 2016). Although there is a screen-printed carbon electrode (SPCE) in conjunction with nano-Prussian blue-chitosan (Guan et al. 2019), it is expensive and challenging to construct. It is important to develop a cost-effective and simple biosensor to detect MC-LR in water.

In this study, an anti-MC-LR/MC-LR/cysteamine-coated screen-printed carbon electrode (SPCE) biosensor was newly fabricated for the detection of MC-LR in real water samples using electrochemical impedance spectroscopy (EIS). Among many antibodies, a specific MC-LR monoclonal antibody was selected due to its high sensitivity and selectivity (Zeck et al. 2001b). The electron transfer properties of the cysteamine functionalized sensor were investigated using cyclic voltammetry (CV). The surface nanolayer of the biosensor was characterized using scanning electron microscopy (SEM)–energy-dispersive X-Ray spectroscopy (EDS) and X-ray photoelectron spectroscopy (XPS). Following the characterization of the anti-MC-LR/MC-LR/cysteamine/SPCE biosensor, the functionality of the sensor's resistance to time and selectivity against other MCs and potentially interfering ions found in surface waters were thoroughly investigated. Finally, the sensor was tested to detect MC-LR in natural surface water samples and compared with previously reported similar methods.

Materials and methods

Chemicals and reagents

Cysteamine (cat. no. M9768) was purchased from Sigma-Aldrich (St. Louis, MO, USA). Sodium phosphate monobasic monohydrate (NaH_2PO_4) (cat. no. 389872500), sodium phosphate dibasic (Na_2HPO_4) (cat. no. 424375000), phosphate buffer saline (PBS) (cat. no. 10010031), potassium Ferricyanide (cat. no. 196785000), sulfo-NHS (N-hydroxysulfosuccinimide) (cat. no. 24510), N-(3-(dimethylamino) propyl)-N′-ethylcarbodiimide hydrochloride (cat. no. 22980), sodium chloride (cat. no. AC447302500), calcium sulfate ($CaSO_4$, cat. no. AA33301A7), cupric sulfate ($CuSO_4$, cat. no. 7758998), and magnesium chloride ($MgCl_2$, cat. no. LC163801) were purchased from Thermo Fisher Scientific (Waltham, MA, USA). MC-LR (cat. no. ALX-350-012-C100), anti-MC-LR monoclonal antibody (MC10E7, lgG1 type, ALX-804-320-C200), MC-YR (cat. no. ALX-350-044-C025), and MC-RR (cat. no. ALX-350-043-C050) were purchased from Enzo Life (Farmingdale, NY, USA). The Abnova™ MC-LR ELISA kit (cat. no. 89028336) was purchased from Thermo Fisher Scientific (Waltham, MA, USA). The ELISA kit was analyzed using a VersaMax microplate reader (Molecular Devices, San Jose, CA, USA).

Phosphate buffer solution (0.01 M) (PB, pH 7.6) was prepared by mixing solutions of NaH_2PO_4 and Na_2HPO_4 in Milli-Q water. The electrolyte solution was prepared by mixing 5 mM $[Fe(CN)_6]^{3-/4-}$ in 10 mM PBS solution (pH 7.3).

Anti-MC-LR/MC-LR/cysteamine/SPCE biosensor fabrication

The surface functionalization process of the anti-MC-LR/MC-LR/cysteamine/SPCE biosensor is shown in Fig. 1. First, the screen-printed carbon electrode (SPCE) (RRPE1001C, Pine Research Instrumentation Inc., Durham NC, USA) was sufficiently cleaned by pouring a small amount (approximately 10 mL) of acetone (99.7%, cat. no. 180349, Thermo Fisher Scientific, Waltham, MA, USA) into individual 50-mL graduated polypropylene centrifuge tubes (cat. no. 14375150, Thermo Fisher Scientific, Waltham, MA, USA), so that the working electrode (WE) was then completely submerged into the solution. With the lid, the tubes were placed in a large beaker with water and a probe-type ultrasonic bath (CL-334, no. 2015060673, Fisher Scientific), making sure none of the tubes were touching either the walls of the beaker or the probe. With a power of 500 W and a frequency of 20 kHz at an amplitude of 25%, the sensors were sonicated for 90 min at room temperature. Then, the sensors were removed and rinsed with 70% isopropanol and Milli-Q water. The sensors were placed in a petri dish with a task wiper (Kimwipes) and dried with N_2 (99.999%). Next, a cysteamine self-assembled monolayer (SAM) was coated onto the surface of the carbon WE to provide anchoring sites for the MC-LR molecules (dos Santos et al. 2019). For the SAM coating, 3 µL of 18 mM cysteamine, diluted using Milli-Q water, was dropped onto the surface of the WE. The sensors were then placed in a dark and semi-humid environment. After 4 h, the electrode was rinsed with Milli-Q water and dried with N_2. To immobilize the MC-LR onto the SAM layer of the WE surface, the WE was incubated with an activated solution of MC-LR. The MC-LR was activated by using equal portions of 20 mM sulfo-N-hydroxysulfosuccinimide (sulfo-NHS), 80 mM N-(3-(dimethylamino) propyl)-N′-ethylcarbodiimide hydrochloride (EDC), and 10^{-2} g L^{-1} of MC-LR and spun in the centrifuge (cat. no. 367160, Beckman Counlter, Inc. (Brea, CA)) at room temperature for 30 min at 500 rpm. Using a pipette, 1 µL of the activated MC-LR solution was dropped onto the WE and allowed to immobilize overnight in the refrigerator (4 °C). The sensor was then rinsed with Milli-Q water and dried with N_2. The fabricated MC-LR detection biosensor was stored in the refrigerator before use (i.e., antibody application to test water samples).

Electrochemical characterization of the MC-LR detection biosensor

The electrochemical characterization of the functionalization process of the Anti-MC-LR/MC-LR/Cysteamine/SPCE biosensor was conducted using EIS and CV measurements performed by the PalmSens 4 (Houten, the Netherlands). Electrochemical characterization was conducted in a three-electrode system using a modified MC-LR/cysteamine/SPCE biosensor as the working electrode (WE), carbon counter electrode, and an Ag/AgCl reference electrode (MI-401, Microelectrodes, Inc., Bedford, NH, USA). The CV and EIS measurements were analyzed for each step of the functionalization process, bare SPCE, cysteamine/SPCE, and MC-LR/cysteamine/SPCE and compared to ensure electrode surface functionalization. For the EIS measurements, the potential of the DC and AC

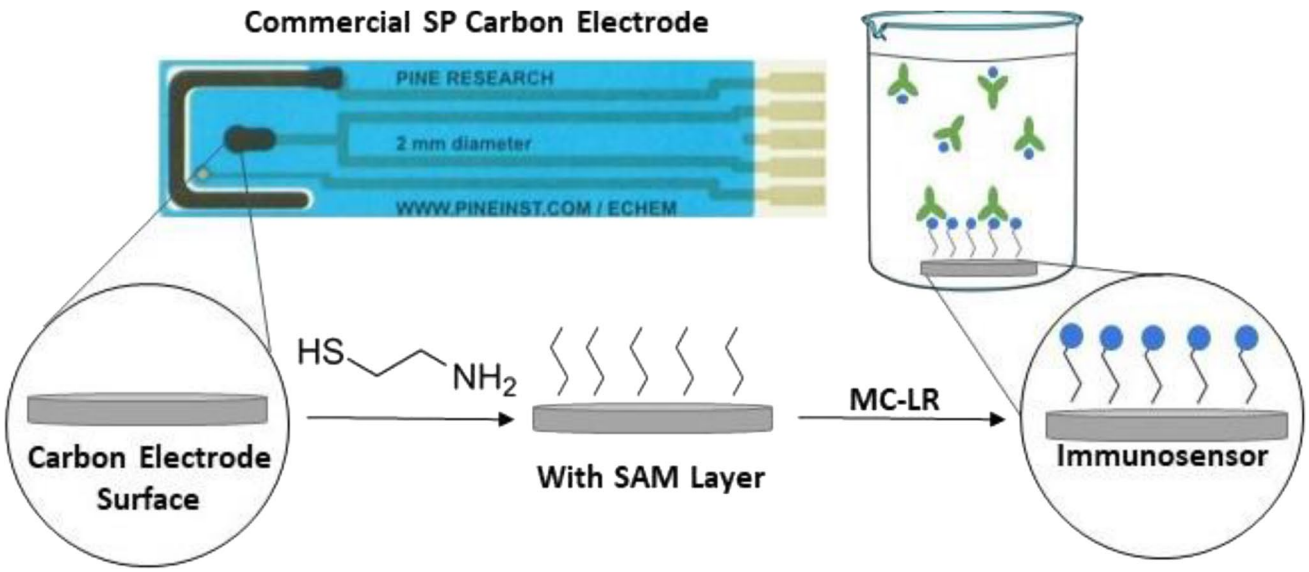

Fig. 1 Surface functionalization of the anti-MC-LR/MC-LR/cysteamine/SPCE biosensor surface and mechanism for the SPCE coated with MC-LR molecules

was set to 0.001 V and 0.250 V, respectively, and a frequency range of 0.01 to 100,000 Hz. For the CV measurements, the *t* equilibrium was set to 8 seconds, the E begin was −1.0 V, the E step was 0.01 V, and the scan rate was 0.05 V s^{-1}.

Surface characterization of the MC-LR detection biosensor using SEM and XPS

Surface structures of the fabricated biosensors were obtained with an Ultra 55 scanning electron microscopy (SEM) (ZEISS, Oberkochen, Germany). To characterize the surface chemical states, X-ray photoelectron spectroscopy (XPS) was performed with a Thermo Scientific ESCALAB Xi+ X-ray Photoelectron Spectrometer Microprobe (Thermo Scientific™, MA, USA) with a twin-crystal, micro-focusing monochromator and an Al anode. The XPS analysis chamber during measurement was held at a pressure below 1.0×10^{-7} torr. All spectra were calibrated to the carbon 1s peak, set to 284.8 eV.

MC-LR detection using the anti-MC-LR/MC-LR/cysteamine/SPCE biosensor

The analytical performance of the biosensor was tested using varying known concentrations of MC-LR. Samples containing concentrations of MC-LR from 10^{-7} to 10^{-4} g L^{-1} were mixed with equal volumes of 10^{-2} g L^{-1} Anti-MC-LR and PB (pH 7.6) using the centrifuge at room temperature for 30 min at 500 rpm. This allows for sufficient time for the antibody to bind to the MC-LR in the sample. One microliter of the sample was then dropped onto the working electrode and let sit, in the closed Petri dish, for an hour at room temperature to allow the available antibody molecules left in solution (not bound to the MC-LR molecules present in the sample) to bind to the MC-LR molecules on the surface of the sensor. The electrode was rinsed with Milli-Q water and then incubated with PB solution for a couple of minutes. The sensor was then tested in the redox probe solution (0.005 M $[Fe(CN)_6]^{3-/4-}$ in PBS) using the PalmSens 4 to obtain EIS graphs. The total whole process including mixing antibodies in the test solution and incubating the sensor took approximately less than 90 min. The peak values (Z_{max}) were obtained from the EIS graph to create the standard curve. The EIS Nyquist plot curves were fitted to the appropriate circuit model using EIS Spectrum Analyser software (ABC Chemistry).

The limit of detection (*LOD*) was calculated using the following equation (Eq. 1) (Lee et al. 2013).

$$LOD = k\frac{S_b}{b} \quad (1)$$

where *k* is the parameter whose value is suggested to be 3 by the International Union of Pure and Applied Chemistry (IUPAC) (Long and Winefordner 1983), S_b is the standard deviation of blank signals, and *b* is the slope of the calibration curve.

The reproducibility of the Anti-MC-LR/MC-LR/Cysteamine/SPCE biosensor was tested by preparing new test solutions and compared to the previously developed standard curve.

The monoclonal antibody (anti-MC-LR) (MC10E7, lgG1 type, ALX-804-320-C200, Enzo Life, Farmingdale, NY, USA) was used because of its high sensitivity and selectivity toward MC-LR (Zeck et al. 2001b). MC10E7 is very stable and exhibits low interferences from humic acid, salts, and surfactants/organic solvents present in solutions (Zeck et al. 2001a), proving it well-suited for its application in a blend of water matrices.

Selectivity and interference tests

The selectivity of the biosensor toward MC-LR was evaluated by testing the cross-reactivity with other common MCs (MC-RR and MC-YR) (Wu et al. 2019). Samples were prepared with a fixed concentration of 10^{-5} g L^{-1} of MC-LR, MC-RR, and MC-YR, as well as a combined sample of three MCs (i.e., MC-LR, MC-RR, and MC-YR).

The interference resilience of the biosensor was also analyzed by adding possible interfering ions commonly found in natural water to the MC-LR test sample. The ions selected for analysis were Na^+, Mg^{2+}, Cu^{2+}, Ca^{2+}, Cl^-, and SO_4^{2-}. In fresh surface water, sodium (Na^+) concentrations typically range between 0 and 100 mg L^{-1}, magnesium (Mg^{2+}) concentration range is 1–100 mg L^{-1}, calcium (Ca^{2+}) concentration range is 1–135 mg L^{-1}, copper (Cu^{2+}) concentration range is 0.5–1,000 µg L^{-1}, chloride (Cl^-) concentration range is 1–100 mg L^{-1}, and sulfate (SO_4^{2-}) concentration averages 53 mg L^{-1} (CEPA 2008; Elbein 2017; Hunt et al. 2012; Morr et al. 2006). Keeping the ion concentrations within the typical ranges of natural surface water, the chemical concentrations selected were 82.4 mg L^{-1} NaCl, 143.4 mg L^{-1} $MgCl_2$, 3.93 mg L^{-1} $CuSO_4$, and 53.7 mg L^{-1} $CaSO_4$. Of MC-LR, 10^{-5} g L^{-1} was tested with the selected concentration of each chemical. A sample was also tested with a mixture of all the chemicals.

Applications to real surface water samples

A natural surface water sample was collected from the Daecheong Lake in South Korea experiencing HAB events (Fig. S1). The sonication method (Kim et al. 2009) was used to lyse the cyanobacteria, ensuring the MC-LR concentrations in the test sample. A CO-Z ultrasonic cleaner (PS-10A, AC100-120V, 60 Hz) was used to sonicate the cyanobacteria for 30 min. The sample was then filtered using a glass fiber prefilter (no. APFA04700, MilliporeSigma, Burlington, MA, USA) to remove the larger particles, and then, a 0.22-µm

membrane filter (no. SLGPM33RS, MilliporeSigma, Burlington, MA, USA) was used to remove the remaining particles. The MC-LR concentration was measured using ELISA (EPA method 546) (Zaffiro et al. 2016) (Supplementary Information (SI) S.1.1.).

Results and discussion

Surface characterization of the fabricated MC-LR detection biosensors

SEM was used to investigate the surface morphology of the electrodes after each step of the sensor surface functionalization (Fig. S2). The bare SPCEs exhibited flakelike carbon structures, several microns in size, accompanied by smaller structures on their surface. These smaller structures include fibers and particles, attributed to polymer binders and fragmented carbon structures typical of electrode fabrication. After each step, the surface modification showed no significant alteration to the structure at the microscale. The density of particle and fibrous structures on the surface seemed to vary, attributed to the commercial SPE fabrication process. No discernible changes can be seen at this scale after functionalization, with surface modifications occurring solely at the nanoscale. All resulting changes to the electrode properties are then attributed to surface functionalization.

XPS confirmed the surface chemical states of the electrodes after surface modification. From the survey spectra and deconvoluted high-resolution spectra, deconvolution of the C 1s and N 1s core-level peaks confirms changes to the chemical states of the surface through the fabrication process (Fig. 2a). Consistent among all C 1s spectra was the presence of the C–C bond peak at 284.8 eV, which was the dominant peak in all electrodes (Fig. 2b). The origin of this peak is from adventitious carbon as well as C–C bonds in coatings on the electrodes. A shorter peak from the C=C moiety at 284.3 eV, which originated from the aromatic carbon of the electrode, was often present. After the coating with cysteamine (i.e., SAM), the signal increased in the region associated with bonds to heteroatoms such as C–N or C–S bonds (Fig. 2b) (Abdul Razzaq et al. 2019). Following the attachment both of MC-LR and anti-MC-LR, the spectra exhibited C–N and C–O bonds, however, showed a signal consistent with amide bonding at 288.4 eV (Ekiz et al. 2011). The electrode after adhesion of Anti-MC-LR did not show the presence of C=C bonding in the deconvolution, likely due to a thickness of the adsorbed layer, where the signal of the carbon electrode was no longer detected as XPS only probes the ~10 nm into the surface (Gilbert et al. 2013).

The N 1s peaks were also deconvoluted to determine the state of nitrogen on the electrode surface (Fig. 2c). In the bare carbon electrode, the XPS indicated charged nitrogen species associated with the peak at ~402.4 eV (Lee et al. 2016). The complex signal likely originated from the binding agents

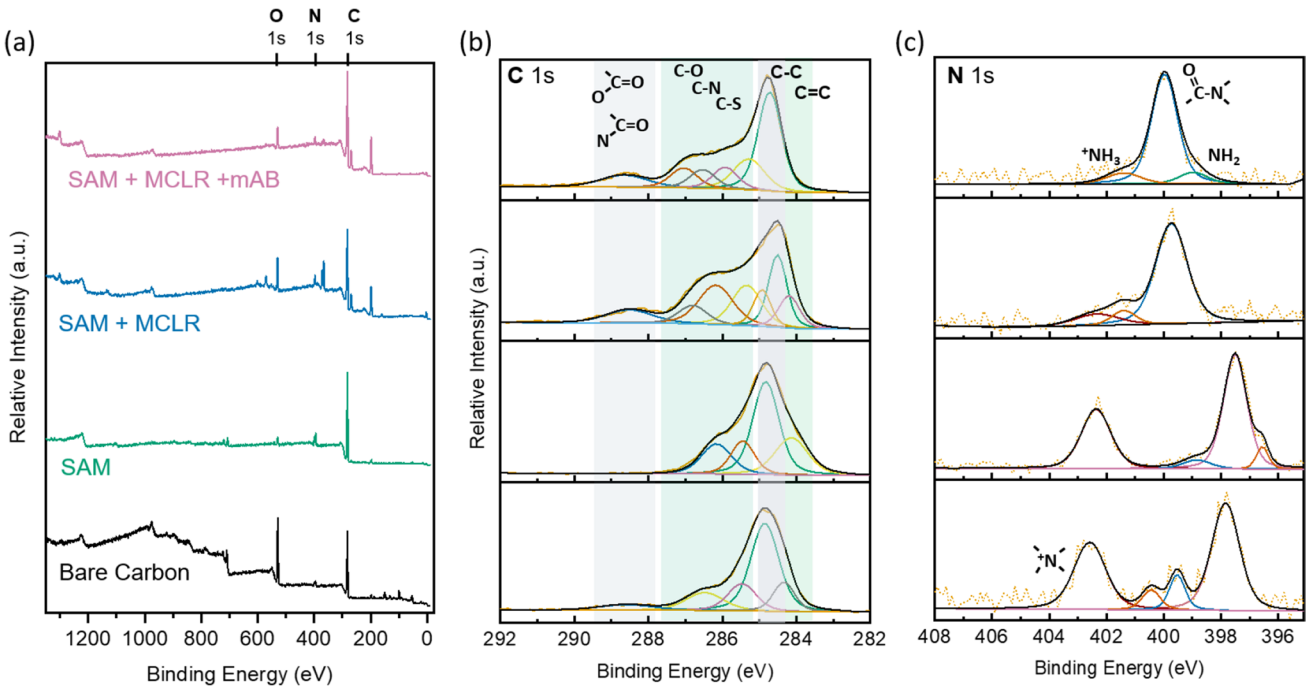

Fig. 2 **a** XPS survey spectra of the SPE through each step of the fabrication process. **b**, **c** High-resolution spectra of the C 1s and N 1s regions for each step. SAM, cysteamine self-assembled monolayer; mAB, monoclonal antibody

applied in commercial electrode fabrication, which can contain charged species such as quaternary nitrogen (Chen et al. 2018; Zhang et al. 2004). The addition of the SAM coating on the electrode shows the emergence of new peaks, with a shoulder often associated with aromatic nitrogen (Yuan et al. 2017), indicating a change to the electrode surface chemistry. After the attachment of the MC-LR, the most prominent peak in the signal appeared at 399.8 eV, indicating the presence of amide bond formation consistent with the chemical structure. MC-LR has several nitrogen-containing functional groups (e.g., amides and guanidine) that further convolute the spectra. After the attachment of Anti-MC-LR, the peak shifts to 400.0 eV, attributed to primary amide bonds, with the shoulders associated with nitrogen in a variety of protonated states (Oh et al. 2013). As was seen in the C 1s spectra, the initial peaks in the N 1s spectra associated with the electrode signal at 402.4 eV are no longer detected after the surface modification process.

Anti-MC-LR/MC-LR/cysteamine/SPCE biosensor electrochemical characterization

The electrode functionalization of the anti-MC-LR/MC-LR/cysteamine/SPCE biosensor was evaluated through the redox behavior of the cysteamine monolayer (i.e., SAM) by CV measurements using the redox probe solution via different substrate layers (Fig. 3a). The highest redox peak current (27 µA) was observed with the SAM layer, which was attributed to the improvement in electron transport due to an electrostatic attraction between the positively charged cysteamine monolayer and the negatively charged redox probe solution (Shervedani et al. 2007). A slight decrease to 20 µA was observed with the addition of the MC-LR, suggesting that binding of the MC-LR acted as a charge insulator from the probe solution and in turn decreases the current response. A lower redox peak (6 µA) was observed for the bare carbon electrode due to the hindrance of electron transport because of the absence of the SAM layer on the working electrode.

The Nyquist plots shown in Fig. 3b were fitted with equivalent circuit models using EIS operation parameters including 0.5 mV and 0.25 V for the DC (direct current) and AC (alternating current), respectively, and a frequency range of 0.01–100 kHz. The bare carbon electrodes (i.e., SPCE) showed the highest peak value of 14 kΩ, indicating the high barrier of electron transfer. The formation of the cysteamine SAM on the electrode generated a layer of high electrostatic attraction (Shervedani et al. 2007) which led to a decrease in

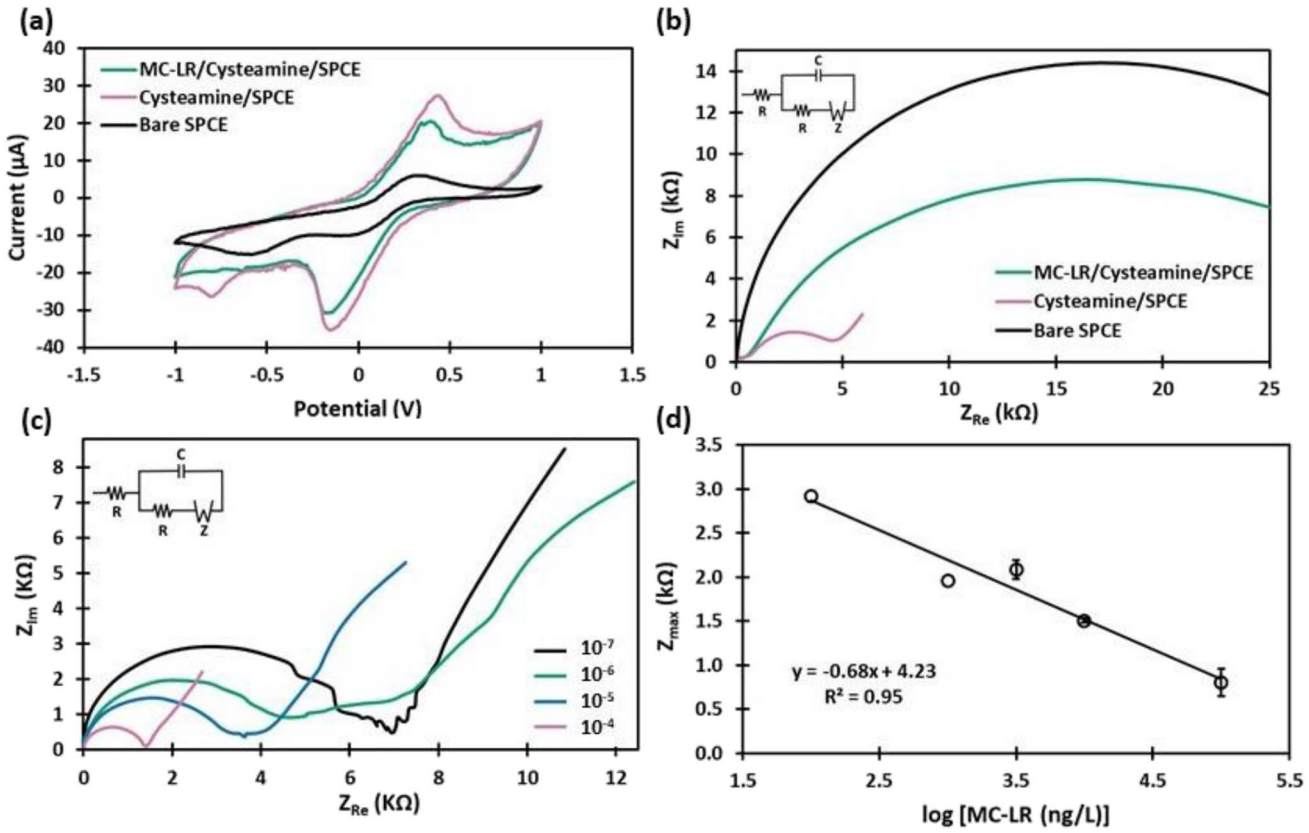

Fig. 3 Anti-MC-LR/MC-LR/cysteamine/SPCE biosensor for MC-LR detection: **a** CV curves, **b** Nyquist plots with different fabrication stages of the sensors, **c** Nyquist plots with different MC-LR concentrations, **d** standardized curve for varying MC-LR test samples with error bars

the peak value to 1.4 kΩ. The immobilization of the MC-LR onto the cysteamine SAM increased the resistance, shown by a higher peak value of 8.7 kΩ on the Nyquist plot, which is in agreement with the result of the CV (Fig. 3a).

Analytical performance of anti-MC-LR/MC-LR/cysteamine/SPCE biosensor

Calibration curve and *LOD*

The purpose of this study was to develop and characterize a cost-effective and simple check for MC-LR in water, based on EIS, using a modified SPCE. The detection strategy was based on an indirect measurement of electron-transfer resistance on the biosensor surface (Han et al. 2013), where MC-LR was covalently immobilized using a cysteamine SAM, and the antibody binding to the MC-LR modified surface was competitively inhibited by MC-LR present in the sample.

EIS measurements were further carried out to characterize the binding between immobilized MC-LR and the anti-MC-LR monoclonal antibody. The variation in the electron-transfer resistance with different concentrations of MC-LR (10^{-7}–10^{-4} g L^{-1}) was evaluated using EIS and a calibration curve was created, where the higher the concentration of MC-LR in the test solution, the lower the number of antibody molecules that were available to attach to the MC-LR on the sensor surface, resulting in a lower electron-transfer resistance. In the Nyquist plots (Fig. 3c), it was obvious that increasing MC-LR concentration caused the decrease of electron transfer impedance on the anti-MC-LR/MC-LR/cysteamine/SPCE biosensor. Therefore, the peak values (Z_{max}) of the Nyquist plot reflect the concentration of antibodies bound on the surface of the electrode in a concentration-dependent manner. These results suggested that the correlation between Z_{max} and MC-LR concentrations can be determined by measuring standard serial dilutions of MC-LR mixed with a constant antibody concentration. Figure 3 d shows the calibration curve, which displays the linearity on MC-LR. The correlation is $Z_{max} = -0.68 \times \log([\text{MC-LR}]) + 4.23$ with $R^2 = 0.95$ for the developed biosensor, where Z_{max} is the peak value observed on the Nyquist plot and [MC-LR] is the concentration of MC-LR (ng/L). The *LOD* was calculated to be 0.69 ng L^{-1}, accomplishing the detection of a much lower concentration than the limit for MC-LR in drinking water guideline of 1 µg L^{-1} according to the WHO and 8 µg L^{-1} for recreational use recommended by the USEPA (USEPA 2019).

Reproducibility was investigated by multiple measurements of certain MC-LR concentrations and plotting the average and standard deviations (Fig. 3d). For the developed MC-LR detection biosensor, MC-LR concentrations of 10^{-4}, 10^{-5}, and $10^{-5.5}$ g L^{-1} had RSD values of 1–19%. These results indicated acceptable reproducibility and feasibility of the biosensors. Another reproducibility test of the anti-MC-LR/MC-LR/cysteamine/SPCE biosensor was conducted using newly prepared solutions. The analysis of the sample with MC-LR concentration of 10^{-5} g L^{-1} showed an error of approximately 3.8% (Fig. 3d). It should be noted that the developed biosensors have been designed to be used as disposable one-time measurements where each measurement uses a new fresh sensor; therefore, inter- and intra-day experiments may not be required for this type of sensor.

The mechanism of EIS detection of MC-LR was based on an inhibition type-immunoassay: The binding of the antibodies to the MC-LR immobilized onto the surface of the electrode was limited by the MC-LR present in the sample that was allowed to react with the antibody before exposure to the sensor. The MC-LR detection concentration range could be shifted to detect higher or lower concentrations by changing the concentration of the antibody. Other solutions to adjust the MC-LR detection ranges can be to increase the size of the working electrode or add nanoparticles to increase the available area in which the MC-LR can be present on the surface, allowing for more bonding sites for the antibody allowing for lower detection limit. However, the current working range seems to be appropriate concerning regulations and typical MC-LR concentrations found in water bodies experiencing HABs.

Selectivity and interference

To evaluate the selectivity of the developed anti-MC-LR/MC-LR/cysteamine/SPCE biosensor against other MCs, samples with equal concentrations of 10^{-5} g L^{-1} of MC-LR and 10^{-5} g L^{-1} of other common MCs (i.e., MC-YR and MC-RR) were tested under the same condition. As shown in Fig. 4a, the electrochemical response for MC-LR including the other MC toxins corresponds to the signal created by the MC-LR sample. The mixed sample (i.e., MC-LR + MC-LR + MC-RR) also showed no significant changes in electron-transfer resistance for MC-LR of 10^{-5} g L^{-1}. The results had an error range of 0.1–6.0% and an RSD range of 10–16%, suggesting high selectivity of the biosensor toward MC-LR.

Specific interference of various possible coexisting ions on the MC-LR detection was also investigated using the developed biosensor. The electrochemical signals of the anti-MC-LR/MC-LR/cysteamine/SPCE biosensor towards the different ions are shown in Fig. 4b. The interfering test results showed that the biosensor has acceptable performance for the measurement of MC-LR for the ion concentrations within the typical ranges of natural surface water. The error range was 1.6–17.7%, and the RSD range was 3–10%, where the most interference was observed for the mixed solution containing all the ions, probably due to increased ion strength. This indicates that higher concentrations of

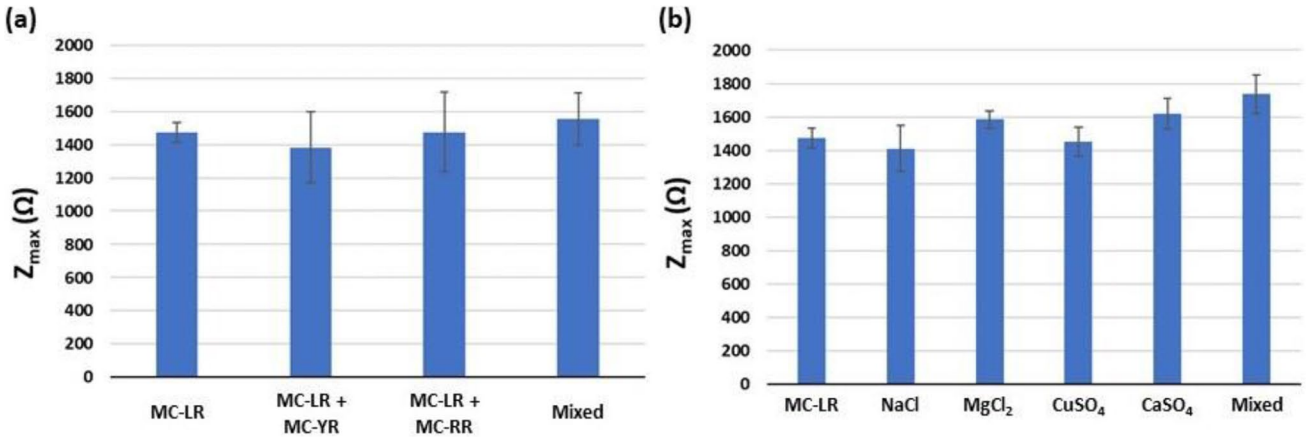

Fig. 4 **a** Selectivity toward other MCs and **b** possible interfering ions effect on the developed biosensor response. MC-LR of 10^{-5} g L^{-1} was included in the sample for the ion interference tests

possible interfering ions may affect the sensor performance. It was found that a higher hardness greater than 180 mg L^{-1} as $CaCO_3$ reduced the accuracy of sensor measurement significantly (~ 67%). Thus, it is highly recommended that a pre-calibration curve be constructed to check the sensor performance before the actual measurements of MC-LR in the water source.

Sensor lifetime

Several biosensors were prepared and tested to determine the shelf-life after development. It was previously reported that gold electrodes for MC-LR detection show good functionality for up the 12 weeks (dos Santos et al. 2019). The carbon-based MC-LR detection biosensors developed in this study were stored in the refrigerator (~4 °C) for 5 and 12 weeks and then tested using the known sample with an MC-LR concentration of 10^{-6} g L^{-1}. The results of the test showed an average error of 16% for 5 weeks and 23% for 12 weeks where the measured resistance of the old sensors was slightly lower than the resistance measured by the sensors tested on the same day as functionalization. However, these results indicate that the sensor has acceptable stability and functionality for up to 12 weeks.

Applications for surface water samples

To evaluate sensor performance in real surface water samples, the anti-MC-LR/MC-LR/cysteamine/SPCE biosensor was investigated for the determination of MC-LR extracted from cyanobacteria in the water experiencing HABs in South Korea. After the cyanobacteria were lysed with sonication and the sample was filtered with a 0.22-µm membrane filter, the MC-LR concentration was determined to be 0.43 µg L^{-1} using ELISA. As the MC-LR concentration from the natural water sample was relatively low to test the biosensor performance, we spiked known MC-LR concentrations to create MC-LR concentrations of 10^{-5}, 10^{-6}, and 10^{-7} g L^{-1} to test the biosensor performance. The MC-LR concentrations in the test samples were also validated using ELISA. From Fig. 5, the anti-MC-LR/MC-LR/cysteamine/SPCE biosensor showed good sensitivity toward MC-LR with well-defined Z_{max} values with different MC-LR concentrations in natural surface water. Similar results of MC-LR detection were observed in the surface water samples with the developed biosensor and ELISA, suggesting a minimal impact on the possible interference of ions (e.g., K^+, Na^+, Cu^{2+}, and Cl^-) during MC-LR detection using the anti-MC-LR/MC-LR/cysteamine/SPCE biosensor. Based on the constructed calibration curve, the natural water sample has an MC-LR concentration of 0.46 µg L^{-1} which is a difference of 6.5% compared to the ELISA test result with an RSD value of 0.64%. Overall, the anti-MC-LR/MC-LR/cysteamine/SPCE biosensor showed good applicability to surface water samples. However, as shown in Fig. 5, it is recommended that

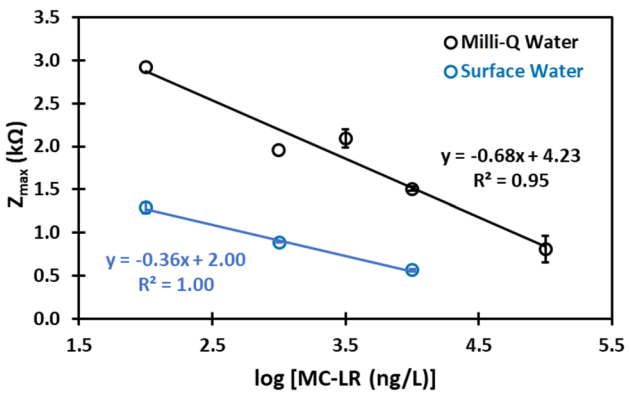

Fig. 5 Standard curve established for Milli-Q water base and surface water base

Table 1 Comparison of studies for MC-LR detection using biosensor technology

Modifier	Analyte	Direct vs. indirect	Detection limit	Mesure mode	Sample tested	References
MC-LR/ctDNA/Au	MC-LR	Direct	1.4 ng/L	EIS	Tap and lake water	Zhang et al. (2018)
MC-LR/ssDNA/Au	MC-LR	Direct	1.8×10^{-11} mol/L	EIS	Lake, river, and tap water	Lin et al. (2013)
MC-LR/MC-LR-A /AgNPs/SDD–Co(II)/GCE	MC-LR	Direct	0.04 µg/L	CV	Freshwater and environmental samples	Bilibana et al. (2016)
HRP-anti-MC-LR/ MC-LR/BSA/anti-MC-LR/AuNR/ MoS_2/Au	HRP-anti-MC-LR	Direct	5 ng/L	DPV	Lake, tap, and drinking water	Zhang et al. (2017)
Au@Pt-anti-MC-LR/MC-LR/anti-MC-LR/AuNCs/ MoS_2/Au	Au@Pt-anti-MC-LR	Direct	0.3 ng/L	DPV	Lake, tap, and drinking water	Pang et al. (2018)
MC-LR/anti-MC-LR/Au NPs/L-cysteine/Au	MC-LR	Direct	20 ng/L	DPV	Lake, tap, and mineral water	Tong et al. (2011)
MC-LR-HRP/ MC-LR/anti-MC-LR/SPGE	MC-LR-HRP	Direct	0.1 ng/L	CV	River water	Campàs and Marty (2007)
MC-LR/anti-MC-LR/AuNP-BSA/ Br-Py/GCE	MC-LR	Direct	0.05 ng/L	EIS	Spiked seawater	Talamini et al. (2018)
$Pt_{70}Ru_{30}$-Ab_2/ MC-LR/BSA/ GS-Ab_1/GCE	$Pt_{70}Ru_{30}$-Ab_2	Direct	9.63 ng/L	CV	Polluted water	Wei et al. (2011)
Au NPs@MIL-101 labeled-MC-LR-BSA/MC-LR/ BSA/anti-MC-LR/ GO/GCE	Au NPs@MIL-101 labeled-MC-LR-BSA	Direct	0.02 µg/L	CV	Lake water	Zhang et al. (2019)
MC-LR/anti-MC-LR/Ag NP/ thiourea SAM/Au	MC-LR	Direct	7.0 pg/L	Capacitance	Bottled, tap, well, reservoir, pond water	Loyprasert et al. (2008)
MC-LR/BSA/anti-MC-LR/Au NP/L-cysteine/Au	MC-LR	Direct	18.2 ng/L	EIS	Bottled water	Sun et al. (2010)
Anti-MC-LR/ MC-LR/cysteamine/Au	Anti-MC-LR	Indirect	0.57 ng/L	EIS	Lake water	dos Santos et al. (2019)
Goat-anti-rabbit(IgG-HRP)/ anti-MC-LR/ MC-LR antigen/ PB-CS/SPCE	Goat-anti-rabbit(IgG-HRP)	Indirect	0.11 ng/L	CV	Spiked tap, reservoir, and lake water	Guan et al. (2019)
HRP-anti-MC-LR/ MC-LR-BSA/ cysteamine-glutaraldehyde/AuNPs/ GCE	HRP-anti-MC-LR	Indirect	4 ng/L	EIS	Lake water	Hou et al. (2016)
AuNPs-Ab_2/anti-MC-LR/MC-LR/ PEG/CNFs/GCE	$AuCl_4^-$	Indirect	1.68 ng/L	DPV	Lake water	Zhang et al. (2016)
HRP-anti-MC-LR/ MC-LR-SWNHs/ GCE	HRP-anti-MC-LR	Indirect	0.03 µg/L	DPV	Lake water	Zhang et al. (2010)

Table 1 (continued)

Modifier	Analyte	Direct vs. indirect	Detection limit	Mesure mode	Sample tested	References
Multi-HRP-(MCSs/Thi@AuNPs)-Ab_2/MC-LR-Ab_1/MC-LR-Ag/GH@PDA/SPCE	Multi-HRP-(MCSs/Thi@AuNPs)-Ab_2	Indirect	9.7 ng/L	CV	Lake water	Gan et al. (2016)
Anti-MC-LR/MC-LR/cysteamine/SPCE	Anti-MC-LR	Indirect	0.69 ng/L	EIS	Lake water	This study

a site-specific calibration curve be constructed periodically to ensure the representativeness of the sensor performance in the water body.

The MC-LR detection performance of the anti-MC-LR/MC-LR/cysteamine/SPCE biosensor was comparable with other sensors which are listed in Table 1. There are two methods for MC-LR detection: direct (Pang et al. 2018; Sun et al. 2010; Wei et al. 2011; Zhang et al. 2019) and indirect (dos Santos et al. 2019; Gan et al. 2016; Guan et al. 2019; Zhang et al. 2010). The direct method uses an antibody bound to the surface to directly measure the amount of MC-LR in the water sample. On the other hand, the indirect method uses MC-LR immobilized onto the surface of the electrode and mixes a known concentration of antibody in the sample and then measures the amount the antibody which binds to the MC-LR on the surface of the electrode. Previous studies (Han et al. 2013) have demonstrated the efficiency of both antibody-coated surfaces and an immobilized MC-LR molecule coating for the detection of MC-LR in water; however, the indirect method is more commonly studied as it provides a lower detection limit (dos Santos et al. 2019; Guan et al. 2019; Hou et al. 2016; Talamini et al. 2018; Tong et al. 2011; Zhang et al. 2017). Previous studies report detection limits are as low as 0.57 ng L^{-1} for gold surface electrodes (dos Santos et al. 2019; Guan et al. 2019; Hou et al. 2016; Lin et al. 2013; Loyprasert et al. 2008; Talamini et al. 2018; Tong et al. 2011; Zhang et al. 2016; Zhang et al. 2018; Zhang et al. 2017). In this study, we also achieved the comparable *LOD* of 0.69 ng L^{-1}. While most biosensors were based on a gold electrode, often with complicated procedures, the developed anti-MC-LR/MC-LR/cysteamine/SPCE biosensor represents a cost-effective and ease of the tool utilization for MC-LR measurements compared to other detection methods (Table S1).

Conclusion

In this study, an anti-MC-LR/MC-LR/Cysteamine/SPCE biosensor has been successfully fabricated and applied for detecting MC-LR in real surface water samples using EIS. The developed method was able to detect MC-LR with excellent sensitivity in complicated surface water samples and has the advantages of a low-cost electrode with reliable performance. Overall, the development of the biosensor has great potential for a sustainable approach to the monitoring of blooms for early action, reducing potential health risks to human. In addition, this study demonstrates an innovative approach to the design and the necessity of cyanotoxin detection due to the health risks associated. The sensor design developed in this study will allow for an on-site, portable, and convenient method of detection while eliminating the need for trained personnel and the time and costs associated with laboratory analysis.

Supplementary Information The online version contains supplementary material available at https://doi.org/10.1007/s11356-022-23300-5.

Acknowledgments The authors acknowledge several fundings (See Funding) and MCF-AMPAC facility, MSE, and CECS.

Author contribution Stephanie Stoll: conceptualization; electrode fabrication; carried out the experiments; formal analysis; experimental investigation; methodology; writing — original draft; writing — review and editing. David Fox: methodology; SEM and XPS analysis; writing — original draft; writing — review and editing. Jae-Hoon Hwang: supervision; methodology; writing — review and editing. Keugtae Kim: sample collection. Lei Zhai: investigation, supervision. Woo Hyoung Lee: conceptualization; investigation; methodology; supervision; writing — original draft; writing — review and editing; supervision.

Funding This work was supported by Korea Environment Industry & Technology Institute (KEITI) through Assessment of the particulate contaminant in wastewater and prediction of their removal efficiency in the wastewater treatment plant Program (or Project), funded by Korea Ministry of Environment (MOE) (RE202101055). This work was supported in part by the U.S. Environmental Protection Agency (USEPA) (Grant Number: SV84002101) and the NSF MRI: EECS: 1726636.

Data Availability Not applicable

Declarations

Ethical approval This is an original article that did not use other information, which requires ethical approval.

Consent to participate All authors participated in this article.

Consent for publication All authors have given consents to the publication of this article.

Competing interests The authors declare no competing interests.

References

Abdul Razzaq A, Yao Y, Shah R, Qi P, Miao L, Chen M, Zhao X, Peng Y, Deng Z (2019) High-performance lithium sulfur batteries enabled by a synergy between sulfur and carbon nanotubes. Energy Storage Mater 16:194–202

Adamovský O, Bláhová L, Kohoutek J, Oravec M, Bláha LJB-VV (2011) Comparison of antibodies commonly used in ELISA for microcystin analyses in natural waters. 47, 5-11

Alipoori S, Rouhi H, Linn E, Stumpfl H, Mokarizadeh H, Esfahani MR, Koh A, Weinman ST, Wujcik EK (2021) Polymer-based devices and remediation strategies for emerging contaminants in water. ACS Appl Polym Mater 3:549–577

Backer L, Manassaram-Baptiste D, LePrell R, Bolton B (2015) Cyanobacteria and algae blooms: review of health and environmental data from the Harmful Algal Bloom-Related Illness Surveillance System (HABISS) 2007–2011. Toxins 7:1048–1064

Bilibana MP, Williams AR, Rassie C, Sunday CE, Makelane H, Wilson L, Ntshongontshi N, Jijana AN, Masikini M, Baker PGL, Iwuoha EI (2016) Electrochemical aptatoxisensor responses on nanocomposites containing electro-deposited silver nanoparticles on poly(propyleneimine) dendrimer for the detection of microcystin-LR in freshwater. Sensors 16:1901

Campàs M, Marty J-LJB, Bioelectronics (2007) Highly sensitive amperometric immunosensors for microcystin detection in algae. 22, 1034-1040

CEPA (2008) Public health goal for copper in drinking water. In: Branch PaET (Hrsg.)

Chen H, Ling M, Hencz L, Ling HY, Li G, Lin Z, Liu G, Zhang S (2018) Exploring chemical, mechanical, and electrical functionalities of binders for advanced energy-storage devices. Chem Rev 118:8936–8982

dos Santos MB, Queirós RB, Geraldes Á, Marques C, Vilas-Boas V, Dieguez L, Paz E, Ferreira R, Morais J, Vasconcelos V (2019) Portable sensing system based on electrochemical impedance spectroscopy for the simultaneous quantification of free and total microcystin-LR in freshwaters. Biosens Bioelectron 142:111550

Dyson K, Huppert DD (2010) Regional economic impacts of razor clam beach closures due to harmful algal blooms (HABs) on the Pacific coast of Washington. Harmful Algae 9:264–271

Ekiz F, Oğuzkaya F, Akin M, Timur S, Tanyeli C, Toppare L (2011) Synthesis and application of poly-SNS-anchored carboxylic acid: a novel functional matrix for biomolecule conjugation. J Mater Chem 21:12337–12343

Elbein A (2017) Lakes are Being A-Salted, Hakai Magazine

Gan C, Sun Z, Ling L, He Z, Lei H, Liu Y (2016) Construction of portable electrochemical immunosensors based on graphene hydrogel@ polydopamine for microcystin-LR detection using multi-mesoporous carbon sphere-enzyme labels. RSC Adv 6:51662–51669

Gilbert JB, Rubner MF, Cohen RE (2013) Depth-profiling X-ray photoelectron spectroscopy (XPS) analysis of interlayer diffusion in polyelectrolyte multilayers. Proc Natl Acad Sci 110:6651–6656

Guan T, Huang W, Xu N, Xu Z, Jiang L, Li M, Wei X, Liu Y, Shen X, Li X (2019) Point-of-need detection of microcystin-LR using a smartphone-controlled electrochemical analyzer. Sensors Actuators B Chem 294:132–140

Han C, Doepke A, Cho W, Likodimos V, de la Cruz AA, Back T, Heineman WR, Halsall HB, Shanov VN, Schulz MJ (2013) a multiwalled-carbon-nanotube-based biosensor for monitoring microcystin-LR in sources of drinking water supplies. Adv Funct Mater 23:1807–1816

Hou L, Ding Y, Zhang L, Guo Y, Li M, Chen Z, Wu X (2016) An ultrasensitive competitive immunosensor for impedimetric detection of microcystin-LR via antibody-conjugated enzymatic biocatalytic precipitation. Sensors Actuators B Chem 233:63–70

Hunt M, Herron E, Green L (2012) Chlorides in fresh water. URI Watershed Watch

Kim IS, Nguyen G-H, Kim S-Y, Lee J-W, Yu H-W (2009) Evaluation of methods for cyanobacterial cell lysis and toxin (microcystin-LR) extraction using chromatographic and mass spectrometric analyses. Environ Eng Res 14:250–254

Lee M-S, Park M, Kim HY, Park S-J (2016) Effects of microporosity and surface chemistry on separation performances of N-containing pitch-based activated carbons for CO2/N2 binary mixture. Sci Rep 6:23224

Lee WH, Wahman DG, Pressman JG (2013) Amperometric carbon fiber nitrite microsensor for in situ biofilm monitoring. Sensors Actuators B Chem 188:1263–1269

Lin Z, Huang H, Xu Y, Gao X, Qiu B, Chen X, Chen G (2013) Determination of microcystin-LR in water by a label-free aptamer based electrochemical impedance biosensor. Talanta 103:371–374

Long GL, Winefordner JD (1983) Limit of detection. A closer look at the IUPAC definition. Anal Chem 55:712A–724A

Loyprasert S, Thavarungkul P, Asawatreratanakul P, Wongkittisuksa B, Limsakul C, Kanatharana P (2008) Label-free capacitive immunosensor for microcystin-LR using self-assembled thiourea monolayer incorporated with Ag nanoparticles on gold electrode. Biosens Bioelectron 24:78–86

Menon S, Mathew MR, Sam S, Keerthi K, Kumar KG (2020) Recent advances and challenges in electrochemical biosensors for emerging and re-emerging infectious diseases. J Electroanal Chem, 114596

Morr S, Cuartas E, Alwattar B, Lane JM (2006) How much calcium is in your drinking water? A survey of calcium concentrations in bottled and tap water and their significance for medical treatment and drug administration. HSS J 2:130–135

Nagata S, Soutome H, Tsutsumi T, Hasegawa A, Sekijima M, Sugamata M, Harada KI, Suganuma M, Ueno YJNt (1995) Novel monoclonal antibodies against microcystin and their protective activity for hepatotoxicity. 3, 78-86

Oh DX, Shin S, Lim C, Hwang DS (2013) Dopamine-mediated sclerotization of regenerated chitin in ionic liquid. Materials 6:3826–3839

Pang P, Teng X, Chen M, Zhang Y, Wang H, Yang C, Yang W, Barrow CJ (2018) Ultrasensitive enzyme-free electrochemical immunosensor for microcystin-LR using molybdenum disulfide/gold nanoclusters nanocomposites as platform and Au@Pt core-shell nanoparticles as signal enhancer. Sensors Actuators B Chem 266:400–407

Park J, Kim KT, Lee WH (2020) Recent advances in information and communications technology (ICT) and sensor technology for monitoring water quality. Water 12:510

Pilevar M, Kim KT, Lee WH (2021) Recent advances in biosensors for detecting viruses in water and wastewater. J Hazard Mater 410:124656

Poretti V, McGeorge L, Miller T, Bryson D, Baldwin-Brown A, Post G, Newby R, Lager L, Schuster R (2020) 2020 cyanobacterial harmful algal bloom (HAB) freshwater recreational response strategy. NJ Department of Environmental Protection

Preece EP, Joan Hardy F, Moore BC, Bryan M (2017) A review of microcystin detections in Estuarine and Marine waters: environmental implications and human health risk. Harmful Algae 61:31–45

Sheng J-W, He M, Shi H-C (2007) A highly specific immunoassay for microcystin-LR detection based on a monoclonal antibody. Anal Chim Acta 603:111–118

Shervedani RK, Farahbakhsh A, Bagherzadeh M (2007) Functionalization of gold cysteamine self-assembled monolayer with ethylenediaminetetraacetic acid as a novel nanosensor. Anal Chim Acta 587:254–262

Shoemaker JA (2015) EPA method 544: determination of microcystins and nodularin in drinking water by SPE and LC-MS/MS detection. In: USEPA O, National Exposure Research Laboratory (Hrsg.)

Sun X, Shi H, Wang H, Xiao L, Li L (2010) A simple, highly sensitive, and label-free impedimetric immunosensor for detection of microcystin-LR in water. Anal Lett 43:533–544

Suo T, Sohail M, Xie S, Li B, Chen Y, Zhang L, Zhang X (2021) DNA nanotechnology: a recent advancement in the monitoring of microcystin-LR. J Hazard Mater 403:123418

Talamini L, Zanato N, Zapp E, Brondani D, Vieira IC (2018) Direct electrochemical nano-immunosensor for microcystin-LR in seawater. Electroanalysis 30:819–827

Tong P, Tang S, He Y, Shao Y, Zhang L, Chen G (2011) Label-free immunosensing of microcystin-LR using a gold electrode modified with gold nanoparticles. Microchim Acta 173:299–305

USEPA (1996) Method 8315A (SW-846): Determination of carbonyl compounds by high performance liquid chromatography (HPLC)

USEPA (2019) Recommended human health recreational ambient water quality criteria or swimming advisories for microcystins and cylindrospermopsin (EPA 822-R-19-001)

Wei Q, Zhao Y, Du B, Wu D, Cai Y, Mao K, Li H, Xu C (2011) Nanoporous PtRu alloy enhanced nonenzymatic immunosensor for ultrasensitive detection of microcystin-LR. Adv Funct Mater 21:4193–4198

Wu X, Hou L, Lin X, Xie Z (2019) Chapter 12 - application of novel nanomaterials for chemo- and biosensing of algal toxins in shellfish and water. In: Wang X, Chen X (eds) Novel nanomaterials for biomedical, environmental and energy applications. Elsevier, pp 353–414

Yuan K, Hu T, Xu Y, Graf R, Shi L, Forster M, Pichler T, Riedl T, Chen Y, Scherf U (2017) Nitrogen-doped porous carbon/graphene nanosheets derived from two-dimensional conjugated microporous polymer sandwiches with promising capacitive performance. Mater Chem Front 1:278–285

Zaffiro A, Rosenblum L, Wendelken SC (2016) Method 546: determination of total microcystins and nodularins in drinking water and ambient water by adda enzyme-linked immunosorbent assay. US EPA (United States Environmental Protection Agency), Standards and Risk Management Division: Cincinnati, OH, USA, 1-21

Zeck A, Eikenberg A, Weller MG, Niessner R (2001a) Highly sensitive immunoassay based on a monoclonal antibody specific for [4-arginine]microcystins. Anal Chim Acta 441:1–13

Zeck A, Eikenberg A, Weller MG, Niessner RJACA (2001b) Highly sensitive immunoassay based on a monoclonal antibody specific for [4-arginine] microcystins. 441, 1-13

Zhang J, Lei J, Xu C, Ding L, Ju H (2010) Carbon nanohorn sensitized electrochemical immunosensor for rapid detection of microcystin-LR. Anal Chem 82:1117–1122

Zhang J, Sun Y, Dong H, Zhang X, Wang W, Chen Z (2016) An electrochemical non-enzymatic immunosensor for ultrasensitive detection of microcystin-LR using carbon nanofibers as the matrix. Sensors Actuators B Chem 233:624–632

Zhang K, Ma H, Yan P, Tong W, Huang X, Chen DD (2018) Electrochemical detection of microcystin-LR based on its deleterious effect on DNA. Talanta 185:405–410

Zhang K, Dai K, Bai R, Ma Y, Deng Y, Li D, Zhang X, Hu R, Yang Y (2019) A competitive microcystin-LR immunosensor based on Au NPs@metal-organic framework (MIL-101). Chin Chem Lett 30:664–667

Zhang SS, Xu K, Jow TR (2004) Evaluation on a water-based binder for the graphite anode of Li-ion batteries. J Power Sources 138:226–231

Zhang Y, Chen M, Li H, Yan F, Pang P, Wang H, Wu Z, Yang W (2017) A molybdenum disulfide/gold nanorod composite-based electrochemical immunosensor for sensitive and quantitative detection of microcystin-LR in environmental samples. Sensors Actuators B Chem 244:606–615